 CMC, vol.9, no.3, pp.179-207, 2009

Identification of dynamical systems with fractional derivative damping models using inverse sensitivity analysis

R Sivaprasad[1,2], **S Venkatesha**[1] **and C S Manohar**[1,3]

Abstract: The problem of identifying parameters of time invariant linear dynamical systems with fractional derivative damping models, based on a spatially incomplete set of measured frequency response functions and experimentally determined eigensolutions, is considered. Methods based on inverse sensitivity analysis of damped eigensolutions and frequency response functions are developed. It is shown that the eigensensitivity method requires the development of derivatives of solutions of an asymmetric generalized eigenvalue problem. Both the first and second order inverse sensitivity analyses are considered. The study demonstrates the successful performance of the identification algorithms developed based on synthetic data on one, two and a 33 degrees of freedom vibrating systems with fractional dampers. Limited studies have also been conducted by combining finite element modeling with experimental data on accelerances measured in laboratory conditions on a system consisting of two steel beams rigidly joined together by a rubber hose. The method based on sensitivity of frequency response functions is shown to be more efficient than the eigensensitivity based method in identifying system parameters, especially for large scale systems.

Keywords: Fractional derivative models; inverse sensitivity analysis; eigenderivatives of asymmetric matrices; system identification.

1 Introduction

The focus of the present study is on inverse problems associated with linear dynamical systems that are governed by equations of the form $M\ddot{x} + C_F D^{\alpha} x + Kx = f(t)$ where t is time, x is a $N \times 1$ vector of system response, a dot represents derivative

[1] Department of Civil Engineering, Indian Institute of Science, Bangalore 560 012 India
[2] General Electric Technology Centre, Bangalore, India
[3] Corresponding author. Email: manohar@civil.iisc.ernet.in; phone: 91 80 2293 3121; fax: 91 80 2360 0404

with respect to time t, M, C_F and K are respectively the $N \times N$ mass, damping and stiffness matrices, $f(t)$ is the external excitation and $D^{\alpha}x(t)$ denotes the α-th order derivative of $x(t)$ with respect to t with α being, in general, a non-integer number. This equation represents the model for linear vibrating systems with fractional order damping model. Specifically, we focus on the problem of characterizing the parameters of the damping force model $CD^{\alpha}x(t)$ based on measured dynamic response of the system.

The problem of characterizing damping in engineering structures has remained one of the challenging problems in structural dynamics (see, for instance, the works of Nashiff *et al.,* 1985, Mallik 1990, Woodhouse 1998, Wineman and Rajagopal 2000, Mead 2000, Jones 2001 and Adhikari 2002, 2005). The value of fractional derivative models in characterizing constitutive laws for rubber like material has been recognized in the existing literature (*e.g.*, Bagley and Torvic 1983a,b, Lee and Tsai 1994, Pritz 1996). Such materials find wide applications in damping treatment and also they appear prominently in the form of hoses in many structures such as an aircraft engine. The paper by Muhr (2007) reviews the mechanics of laminates of elastomer and shims of high modulus and considers questions on damping imparted by rubber to metallic panels. An understanding of dynamic magnification of response in such structures requires insights into damping characteristics of structural elements made up of rubber like material. It has been recognized that models with fractional derivative terms in their equation of motion offer a parsimonious means for capturing the frequency dependent constitutive behavior of viscoelastic material. Studies on solution of fractional order differential equations that arise in structural dynamics are also available: some of the techniques studied include method of Adomian decomposition (e.g., Ray *et al.,* 2005), method of iterations (*e.g.*, Ingman and Suzdalnitsky 2001), and transform techniques (e.g., Bagley and Torvic 1983, Maia *et al.,* 1998). The response of these systems to random excitations has also been explored (*e.g.*, Spanos and Zeldin 1997 and Agarwal 2001).

While the forward problem of analyzing the response of systems with fractional derivative terms has received wide attention, the inverse problem of identifying model parameters from measured responses has not received as much attention. In this context it may be noted that the problem of identification of damping in systems with viscous and structural damping models is extensively studied in the existing literature. Thus, the traditional modal analysis methods routinely extract modal characteristics from measured frequency response or impulse response functions (Ewins 2000, Maia and Silva 1997). Methods based on inverse sensitivity of complex valued eigensolutions and sensitivity of frequency response functions have been developed for problems of structural system identification and vibration based damage detection (e.g., Nobari 1991, Lin *et al.,* 1994,1995, Lee and Kim

2001, Choi *et al.,* 1994a,b, Maia *et al.,* 2003). In a recent paper Reddy and Ganguli (2007) have employed Fourier analysis of mode shapes and have introduced a damage index in terms of vector of Fourier coefficients. A related inverse problem of estimating applied time dependent forces on a beam using an iterative regularization scheme has been investigated by Huang and Shih (2007). Characterization of degradation in composite beams using a wave based approach that employs wavelet based spectral finite element scheme has been developed by Tabrez *et al.,* (2007).

The extension of the tools based on sensitivity of eigensolutions and FRF-s to systems with fractional order damping models appears to have not been considered in the existing literature. Accordingly, we focus in the present study on identifying parameters of dynamical systems with fractional order damping models based on inverse sensitivity analysis of eigensolutions and FRF-s. In this case the eigensolutions are known to be damping dependent, complex valued and are obtained as solutions of a generalized asymmetric eigenvalue problem. The order of the eigenvalue problem is shown to depend upon dynamical degree of freedom of the system and also on the order of the fractional derivative. The FRF based method is shown to be conceptually simpler and more generally valid. The study demonstrates the successful performance of the identification algorithms developed based on synthetic data on one, two and a 33 degrees of freedom vibrating systems. Limited studies, with mixed success, have also been conducted by combining finite element modeling with experimental data on accelerances measured in laboratory conditions on a system consisting of two steel beams rigidly joined together by a rubber hose.

2 Frequency response function and system normal modes

We consider a N-dof dynamical system governed by the equation

$$M\ddot{x}+C\dot{x}+C_F D^{\alpha}x+Kx=F(t) \tag{1}$$

Here t is time, x is a $N\times 1$vector of system response, a dot represents derivative with respect to time t, M, C, C_F and K are respectively the $N\times N$ mass, viscous damping, fractional damping and stiffness matrices, $F(t)$ is the external excitation and $D^{\alpha}x(t)$ denotes the α-th order derivative of $x(t)$ with respect to t with α being, in general, a fractional number. Following Oldham and Spanier (1974), we define $D^{\alpha}x(t)$ as

$$D^{\alpha}x(t)=\frac{d^{\alpha}x}{dt^{\alpha}}=\frac{1}{\Gamma(1-\alpha)}\int_0^t \frac{x(z)}{(t-z)^{\alpha}}dz \tag{2}$$

Here $\Gamma(\cdot)$ is the gamma function. We focus in this study on normal mode oscillations and steady state harmonic responses of the system governed by equation 1. Thus, if $F(t) = F_0 \exp(i\omega t)$, for $t \to \infty$, one could seek the solution of equation 1 in the form $x(t) = X(\omega)\exp(i\omega t)$ and deduce

$$X(\omega) = \left[-\omega^2 M + i\omega C + (i\omega)^{\alpha} C_F + K\right]^{-1} F_0 \exp(i\omega t) \tag{3}$$

Here $H(\omega) = D^{-1}(\omega) = \left[-\omega^2 M + i\omega C + (i\omega)^{\alpha} C_F + K\right]^{-1}$ is the system frequency response function, which, in the present case is also termed as receptance; the matrix $D(\omega)$ is the system dynamic stiffness matrix (DSM). If response velocity and accelerations are sought, one gets $\dot{x}(t) = i\omega X(\omega)\exp(i\omega t)$ and $\ddot{x}(t) = -\omega^2 X(\omega)\exp(i\omega t)$ and the quantities $Y(\omega) = -i\omega H(\omega)$ and $A(\omega) = -\omega^2 H(\omega)$ are respectively known as mobility and accelerance functions. In deriving equation 3, use has been made of the relation $D^{\alpha}[\exp(i\omega t)] = (i\omega)^{\alpha}\exp(i\omega t)$. The elements of $H(\omega)$ could also be derived as a series in terms of system eigensolutions. This is possible, for example, when we write $\alpha = 1/q$ where q is an integer. To demonstrate this we rewrite equation 1 as

$$D^{\frac{2q}{q}} x + M^{-1} C D^{\frac{q}{q}} x + M^{-1} C_F D^{\frac{1}{q}} x + M^{-1} K D^0 x = M^{-1} F(t) \tag{4}$$

This can be recast into a general form as

$$a_{2q} D^{\frac{2q}{q}} x + a_{2q-1} D^{\frac{2q-1}{q}} x + \cdots + a_0 D^{\frac{0}{q}} x = f(t) \tag{5}$$

Here $\{[a_i]\}_{i=0}^{2q}$ are $N \times N$matrices; depending on the value of q, a subset of these matrices would be zero matrices. Thus, for $q = 3$, one gets

$$a_6 D^{\frac{6}{3}} x + a_5 D^{\frac{5}{3}} x + \cdots + a_0 D^{\frac{0}{3}} x = f(t) \tag{6}$$

with $[a_6] = I$, $[a_5] = [a_4] = [a_2] = 0$, $[a_3] = [M^{-1}C]$ and $[a_0] = [M^{-1}K]$. It can be shown that by introducing a $2Nq \times 1$ state vector z equation can be cast in the form

$$A D^{\frac{1}{q}} z - Bz = f(t) \tag{7}$$

where A and B are $2Nq \times 2Nq$ asymmetric, sparse matrices.To illustrate this, we consider q=3 and N=2, and, in this case, equation 7 reads as $AD^{\frac{1}{3}} z - Bz = f(t)$ with

$$z = \begin{Bmatrix} D^{\frac{5}{3}} x \\ D^{\frac{4}{3}} x \\ D^{\frac{3}{3}} x \\ D^{\frac{2}{3}} x \\ D^{\frac{1}{3}} x \\ D^{\frac{0}{3}} x \end{Bmatrix}_{12\times 1} \tag{8a}$$

$$A = \begin{bmatrix} [0] & [0] & [0] & [0] & [0] & [I] \\ [0] & [0] & [0] & [0] & [I] & [0] \\ [0] & [0] & [0] & [I] & [0] & [0] \\ [0] & [0] & [I] & [0] & [0] & [0] \\ [0] & [I] & [0] & [0] & [0] & [0] \\ [I] & [0] & [0] & [a'_3] & [a'_2] & [a'_1] \end{bmatrix}_{12\times 12} \tag{8b}$$

$$B = \begin{bmatrix} [0] & [0] & [0] & [0] & [I] & [0] \\ [0] & [0] & [0] & [I] & [0] & [0] \\ [0] & [0] & [I] & [0] & [0] & [0] \\ [0] & [I] & [0] & [0] & [0] & [0] \\ [I] & [0] & [0] & [0] & [0] & [0] \\ [0] & [0] & [0] & [0] & [0] & [-a'_0] \end{bmatrix}_{12\times 12} \tag{8c}$$

where, $[a'_5] = [a'_4] = [a'_2] = 0$, $[a'_3] = [M]^{-1}[C_2]$, $[a'_1] = [M]^{-1}[C_1]$ and $[a'_0] = [M]^{-1}[K]$ are 2×2 matrices and $\{f(t)\} = [M]^{-1}\{F(t)\}$. Clearly, given that the matrices A and B are asymmetric, the equations for $\{z_i\}_{i=1}^{2Nq}$ (equation 7) would be mutually coupled. We seek a transformation of the coordinates which would uncouple these equations and, towards reaching this end, we seek special free vibration the solution of equation $AD^{\frac{1}{3}}z - Bz = 0$ of the form $z = \psi \exp(\lambda t)$. This leads to the eigenvalue problem

$$B\psi = \lambda A\psi \tag{9}$$

This further leads to *2Nq* eigenpairs and, since the matrices A and B here are asymmetric, the eigenvalues and eigenvectors are in general complex valued. By taking conjugation on both sides of equation 9 it can be verified that these eigensolutions appear in pairs of complex conjugates. To proceed further, we also consider the eigenvalue problem associated with the transpose of matrices A and B given by

$$B^t\phi = \mu A^t\phi \tag{10}$$

It can be verified that $\lambda = \mu$ the eigenvectors ϕ and ψ satisfy the orthogonality relations given by

$$\phi_s^t A\psi_r = \delta_{rs}; \quad \phi_s^t B\psi_r = \lambda_r\delta_{rs} \tag{11}$$

Here δ_{rs} is the Kronceker's delta function and f_r and y_s are respectively the r-th left and s-th right eigenvectors. By introducing the modal matrices $\Phi = [\phi_{rs}]$ and $\Psi = [\psi_{rs}]$ with $r,s = 1,2,\cdots,2Nq$, and suitably normalizing the eigenvectors with respect to A matrix, we can rewrite the above orthogonality relations as

$$\Phi^t A\Psi = I \quad \text{and} \quad \Phi^t B\Psi = \Lambda \tag{12}$$

Here Λ is a $2Nq \times 2Nq$ diagonal matrix with the diagonal elements being equal to the eigenvalues $\lambda_i, i = 1,2,\cdots,2Nq$. Now, returning to equation 7, we introduce the transformation $z(t) = \Psi u(t)$ which leads to the equation

$$A\Psi D^{\frac{1}{q}} u - B\Psi u = f(t) \tag{13}$$

Pre-multiplying the above equation by Φ^t and utilizing the orthogonality relations (12), the above equation can be shown to lead to the following set of uncoupled fractional order differential equations

$$D^{\frac{1}{q}} u_n - \lambda_n u_n = p_n \exp(i\omega t); \quad n = 1,2,\cdots 2Nq \tag{14}$$

Here $\{p_n\} = \Phi^t F_0$ is the amplitude of the generalized force. Based on this we obtain the steady state harmonic response of the system in the original coordinate system as

$$z_k(t) = \sum_{n=1}^{2Nq} \frac{p_n \Psi_{kn}}{(i\omega)^{\frac{1}{q}} - \lambda_n} \exp(i\omega t) \tag{15}$$

If all the terms in the above modal expansion are retained, the resulting solution is expected to lead to results that are identical with those obtained from equation 3.

It may also be noted here that the eigensolutions Λ, Φ and Ψ possess specific internal structure which needs to be recognized in modeling work. To demonstrate this we again consider the eigensolutions for the case of q=3 and N=2 (equation 6). For the s-th mode, if we write $x(t) = \gamma_s \exp(\lambda_s t)$ where γ_s is a $N \times 1$ vector extracted from Ψ, it follows from equation 8a that the s-th eigenvector need to be of the form

$$\psi_s = \left[\lambda_s^{\frac{5}{3}}\gamma_s \quad \lambda_s^{\frac{4}{3}}\gamma_s \quad \lambda_s^{\frac{3}{3}}\gamma_s \quad \lambda_s^{\frac{2}{3}}\gamma_s \quad \lambda_s^{\frac{1}{3}}\gamma_s \quad \gamma_s\right]^t \tag{16}$$

Since, eigensolutions appear in conjugate pairs, it follows that the following is also an eigenvector

$$\psi_s^* = \left[\lambda_s^{*\frac{5}{3}}\gamma_s^* \quad \lambda_s^{*\frac{4}{3}}\gamma_s^* \quad \lambda_s^{*\frac{3}{3}}\gamma_s^* \quad \lambda_s^{*\frac{2}{3}}\gamma_s^* \quad \lambda_s^{*\frac{1}{3}}\gamma_s^* \quad \gamma_s^*\right]^t \tag{17}$$

A similar representation for the right vector ϕ_s is also possible and we denote by ρ_s the $N \times 1$ extract of Φ on lines similar to the definition ofγ_s. Consequently, the

matrices Φ and Ψ will have the form

$$\Psi = \begin{bmatrix} \chi\beta^{\frac{5}{3}} & \chi^*\beta^{*\frac{5}{3}} \\ \chi\beta^{\frac{4}{3}} & \chi^*\beta^{*\frac{4}{3}} \\ \chi\beta^{\frac{3}{3}} & \chi^*\beta^{*\frac{3}{3}} \\ \chi\beta^{\frac{2}{3}} & \chi^*\beta^{*\frac{2}{3}} \\ \chi\beta^{\frac{1}{3}} & \chi^*\beta^{*\frac{1}{3}} \\ \chi & \chi^* \end{bmatrix}; \quad \Phi = \begin{bmatrix} \vartheta\beta^{\frac{5}{3}} & \vartheta^*\beta^{*\frac{5}{3}} \\ \vartheta\beta^{\frac{4}{3}} & \vartheta^*\beta^{*\frac{4}{3}} \\ \vartheta\beta^{\frac{3}{3}} & \vartheta^*\beta^{*\frac{3}{3}} \\ \vartheta\beta^{\frac{2}{3}} & \vartheta^*\beta^{*\frac{2}{3}} \\ \vartheta\beta^{\frac{1}{3}} & \vartheta^*\beta^{*\frac{1}{3}} \\ \vartheta & \vartheta^* \end{bmatrix} \tag{18}$$

Here χ and ϑ are $N \times N$ matrices with $\chi = [\gamma_s]; s = 1,2,\cdots N$ and $\vartheta = [\rho_s]; s = 1,2,\cdots N$ and β is a diagonal matrix of size $N_q \times N_q$ with diagonal entries containing $\lambda_s; s = 1,2,\cdots,N_q$. It may be noted in this context that a similar partitioning of modal matrix is generally done for damped normal modes of viscously damped systems.

3 Sensitivity analysis

Let $p = \{p_i\}_{i=1}^n$ denote a set of system parameters which we wish to identify from the free vibration response and harmonic forced vibration characteristics. As a first step in addressing this identification problem, we need to determine the derivative(s) of the FRF-s and the eigensolutions with respect to $\{p_i\}_{i=1}^n$.

3.1 FRF sensitivity analysis

In order to find $\frac{\partial H}{\partial p_i}$, we define $\Omega(\omega) = H^{-1}(\omega)$ and consider the relation $H(\omega)\Omega(\omega) = I$. From this it follows

$$\frac{\partial H}{\partial p_i}\Omega(\omega) + H(\omega)\frac{\partial \Omega}{\partial p_i} = 0 \tag{19}$$

leading to

$$\frac{\partial H}{\partial p_i} = -H(\omega)\frac{\partial \Omega}{\partial p_i}\Omega^{-1}(\omega) = -H(\omega)\frac{\partial \Omega}{\partial p_i}H(\omega) \tag{20}$$

Noting that $\Omega(\omega) = \left[-\omega^2 M + i\omega C + (i\omega)^\alpha C_F + K\right]$, we get

$$\frac{\partial H}{\partial p_i} = -H(\omega)\left[-\omega^2\frac{\partial M}{\partial p_i} + (i\omega)^\alpha\frac{\partial C_F}{\partial p_i} + i\omega\frac{\partial C}{\partial p_i} + \frac{\partial K}{\partial p_i}\right]H(\omega) \tag{21}$$

Higher order derivatives, if desired, could be obtained by differentiating the above equation further. Thus, by differentiating with respect to p_j, it can be shown that

$$\frac{\partial^2 H}{\partial p_i \partial p_j} = -\left[\frac{\partial H}{\partial p_j}\frac{\partial \Omega}{\partial p_i}H(\omega) + H(\omega)\frac{\partial^2 \Omega}{\partial p_i \partial p_j}H(\omega) + H(\omega)\frac{\partial \Omega}{\partial p_i}\frac{\partial H}{\partial p_j}\right] \tag{22}$$

with

$$\frac{\partial^2\Omega}{\partial p_i \partial p_j} = \left[-\omega^2 \frac{\partial^2 M}{\partial p_i \partial p_j} + (i\omega)^\alpha \frac{\partial^2 C_F}{\partial p_i \partial p_j} + i\omega \frac{\partial^2 C}{\partial p_i \partial p_j} + \frac{\partial^2 K}{\partial p_i \partial p_j}\right] \tag{23}$$

Remarks

It is possible that the parameter α itself could be one of the parameters belonging to the set $\{p_i\}_{i=1}^n$. In this case the deduction of $\frac{\partial\Omega}{\partial p_i}$ and $\frac{\partial^2\Omega}{\partial p_i \partial p_j}$ needs to take cognizance of this possibility.

The structural matrices M, C, C_F and K often could be linear functions of parameters $\{p_i\}_{i=1}^n$ In this case the term $\frac{\partial^2\Omega}{\partial p_i \partial p_j}$ would be zero thereby affording further simplification of equation 22 .

3.2 Eigensensitivity analysis

In order to derive the sensitivity of eigensolutions, we begin by introducing the notation $F_r = B - \lambda_r A$ so that the underlying eigenvalue problems can be written as $F_r \psi_r = 0$ and $\phi_r^t F_r = 0$. From this it follows, $\phi_r^t F_r \psi_r = 0$ which, in turn, leads to the equation

$$\frac{\partial \phi_r^t}{\partial p_j} F_r \psi_r + \phi_r^t \frac{\partial F_r}{\partial p_j} \psi_r + \phi_r^t F_r \frac{\partial \psi_r}{\partial p_j} = 0 \tag{24}$$

Noting that $F_r \psi_r = 0$ and $\phi_r^t F_r = 0$, the above equation is simplified to get

$$\phi_r^t \left[\frac{\partial B}{\partial p_j} - \frac{\partial \lambda_r}{\partial p_j} A - \lambda_r \frac{\partial A}{\partial p_j}\right] \psi_r = 0 \tag{25}$$

Here, by virtue of the normalization condition we have $\phi_r^t A \psi_r = 1$, leading to

$$\frac{\partial \lambda_r}{\partial p_j} = \phi_r^t \left[\frac{\partial B}{\partial p_j} - \lambda_r \frac{\partial A}{\partial p_j}\right] \psi_r \tag{26}$$

The derivatives of ψ_r and ϕ_r with respect to p_j can be obtained by considering the equations $F_r \psi_r = 0$ and $\phi_r^t F_r = 0$, from which one gets

$$\frac{\partial F_r}{\partial p_j} \psi_r + F_r \frac{\partial \psi_r}{\partial p_j} = 0 \text{ and } \frac{\partial F_r^t}{\partial p_j} \phi_r + F_r^t \frac{\partial \phi_r}{\partial p_j} = 0 \tag{27}$$

leading to the approximations

$$\begin{aligned} \frac{\partial \psi_r}{\partial p_j} &= -F_r^+ \left[\frac{\partial B}{\partial p_j} - \frac{\partial \lambda_r}{\partial p_j} A - \lambda_r \frac{\partial A}{\partial p_j}\right] \psi_r \\ \frac{\partial \phi_r}{\partial p_j} &= -[F_r^t]^+ \left[\frac{\partial B^t}{\partial p_j} - \frac{\partial \lambda_r}{\partial p_j} A^t - \lambda_r \frac{\partial A^t}{\partial p_j}\right] \phi_r \end{aligned} \tag{28}$$

Here the superscript + denotes the matrix pseudo-inverse operation. Further modification to these gradients can be derived by considering additional equations arising out of orthogonality relations. Thus, for two distinct eigenpairs we have

$$\phi_s^t B \psi_r = \delta_{rs}; \quad \text{and} \quad \phi_s^t A \psi_r = \lambda_r \delta_{rs} \tag{29}$$

Differentiating these equations with respect to p_j, we get

$$\begin{aligned} &\frac{\partial \phi_s^t}{\partial p_j} B \psi_r + \phi_s^t \frac{\partial B}{\partial p_j} \psi_r + \phi_s^t B \frac{\partial \psi_r}{\partial p_j} = 0 \\ &\frac{\partial \phi_s^t}{\partial p_j} A \psi_r + \phi_s^t \frac{\partial A}{\partial p_j} \psi_r + \phi_s^t A \frac{\partial \psi_r}{\partial p_j} = \frac{\partial \lambda_r}{\partial p_j} \delta_{rs} \end{aligned} \tag{30}$$

Noting that $\frac{\partial \phi_s^t}{\partial p_j} B \psi_r$ and $\frac{\partial \phi_s^t}{\partial p_j} A \psi_r$ are scalars, and hence could be replaced respectively by $\psi_r^t B^t \frac{\partial \phi_s}{\partial p_j}$ and $\psi_r^t A^t \frac{\partial \phi_s}{\partial p_j}$, the above equation can be written as

$$\begin{aligned} &\psi_r^t B^t \frac{\partial \phi_s}{\partial p_j} + \phi_s^t \frac{\partial B}{\partial p_j} \psi_r = -\phi_s^t B \frac{\partial \psi_r}{\partial p_j} \\ &\psi_r^t A^t \frac{\partial \phi_s}{\partial p_j} + \phi_s^t \frac{\partial A}{\partial p_j} \psi_r = -\phi_s^t A \frac{\partial \psi_r}{\partial p_j} + \frac{\partial \lambda_r}{\partial p_j} \delta_{rs} \end{aligned} \tag{31}$$

Combining these equations with equation 27 it can be shown that

$$\begin{Bmatrix} \frac{\partial f_s}{\partial p_j} \\ \frac{\partial y_r}{\partial p_j} \end{Bmatrix} = \begin{bmatrix} F_s^t & 0 \\ 0 & F_r \\ y_r^t B^t & f_s^t B \\ y_r^t A^t & f_s^t A \end{bmatrix} + \begin{Bmatrix} -\frac{\partial F_s^t}{\partial p_j} f_s \\ -\frac{\partial F_r}{\partial p_j} y_r \\ -f_s^t \frac{\partial B}{\partial p_j} y_r \\ -f_s^t \frac{\partial A}{\partial p_j} y_r + \frac{\partial \lambda_r}{\partial p_j} d_{rs} \end{Bmatrix} \tag{32}$$

Clearly, more elaborate equations for the eigenvector derivatives could be derived by considering orthogonality relationship between more than one pair of eigenvectors: these details are available in the thesis by Venkatesha (2007).

Higher order eigenvalue derivatives, if desired, could now be derived as

$$\begin{aligned} \frac{\partial^2 \lambda_r}{\partial p_i \partial p_j} = \frac{\partial \phi_r^t}{\partial p_i} \left[\frac{\partial B}{\partial p_j} - \lambda_r \frac{\partial A}{\partial p_j} \right] \psi_r + \phi_r^t \left[\frac{\partial^2 B}{\partial p_i \partial p_j} - \frac{\partial \lambda_r}{\partial p_i} \frac{\partial A}{\partial p_j} - \lambda_r \frac{\partial^2 A}{\partial p_i \partial p_j} \right] \psi_r \\ + \phi_r^t \left[\frac{\partial B}{\partial p_j} - \lambda_r \frac{\partial A}{\partial p_j} \right] \frac{\partial \psi_r}{\partial p_i} \end{aligned} \tag{33}$$

Similarly, for eigenvectors, a first level of formulation based on equation 28 leads to

$$\begin{aligned}\frac{\partial^2\psi_r}{\partial p_i\partial p_j} &= -F_r^+\left[\frac{\partial^2 F_r}{\partial p_i\partial p_j}\psi_r+\frac{\partial F_r}{\partial p_j}\frac{\partial\psi_r}{\partial p_i}+\frac{\partial F_r}{\partial p_i}\frac{\partial\psi_r}{\partial p_j}\right]\\ \frac{\partial^2\phi_r}{\partial p_i\partial p_j} &= -[F_r^t]^+\left[\frac{\partial^2 F_r^t}{\partial p_i\partial p_j}\phi_r+\frac{\partial F_r^t}{\partial p_j}\frac{\partial\phi_r}{\partial p_i}+\frac{\partial F_r^t}{\partial p_i}\frac{\partial\phi_r}{\partial p_j}\right]\end{aligned} \tag{34}$$

Again, by considering orthogonality relations between two or more distinct eigenvectors, more elaborate equations for these derivatives could be deduced: we omit these details.

4 Inverse sensitivity analysis

Let $\Gamma_k(p_1,p_2,\cdots,p_n);\ k=1,2,\cdots,N_k$ denote a specific set of dynamic characteristics of the system which could be measured. This, for instance, could include a set of eigensolutions or a set of FRF-s at a set of frequencies. The objective of inverse sensitivity analysis is to determine the parameters $\{p_i\}_{i=1}^n$ based on the observed values of $\Gamma_k(p_1,p_2,\cdots,p_n);k=1,2,\cdots,N_k$ and based on the availability of a mathematical model for the system behavior. This model is presumed to be capable of depicting the behavior of the system accurately if the model parameters are assigned the "correct" values. Also it is assumed that the response characteristics $\Gamma_k(p_1,p_2,\cdots,p_n);k=1,2,\cdots,N_k$ are differentiable with respect to the parameters $\{p_i\}_{i=1}^n$ to a desired level. Let $p_u=\{p_{ui}\}_{i=1}^n$ denote the initial guess on the model parameters so that an improved estimate of p could be obtained as $p_{di}=p_{ui}+\Delta_i, i=1,2,\cdots,n$ where Δ_i is the correction to the i-th system parameter. Based on Taylor's expansion, we can write

$$\begin{aligned}\Gamma_k(p_{u1}+\Delta_1,p_{u2}+\Delta_2,\ldots,p_{un}+\Delta_n) &= \Gamma_k(p_{u1},p_{u2},\ldots,p_{un})+\sum_{i=1}^n\left.\frac{\partial\Gamma_k}{\partial p_i}\right|_{p=p_u}\Delta_i\\ &+\frac{1}{2}\sum_{i=1}^n\sum_{j=1}^n\left.\frac{\partial^2\Gamma_k}{\partial p_i\partial p_j}\right|_{p=p_u}\Delta_i\Delta_j+\cdots;\quad k=1,2,\cdots,N_k\end{aligned} \tag{35}$$

Here $\Gamma(p_u+\Delta)$ is interpreted as the observed characteristic from measurements and $\Gamma(p_u)$ is taken to be the prediction of Γ based on the mathematical model with $p=p_u$. The first and second order gradients appearing in the above equation can be deduced from the initial mathematical model using formulation presented in the preceding section. In a *first* order inverse sensitivity analysis we retain only the first two terms in the above equation and obtain

$$\Delta\Gamma_k=\Gamma_k(p_u+\Delta)-\Gamma_k(p_u)=\sum_{i=1}^n\left.\frac{\partial\Gamma_k}{\partial p_i}\right|_{p=p_u}\Delta_i;\quad k=1,2,\cdots,N_k \tag{36}$$

In matrix notation this can be written as

$$\{\Delta\Gamma\} = [S]\{\Delta\} \tag{37}$$

which represents a set of N_k equations in n unknowns. It is assumed that $N_k > n$ and, consequently, an optimal estimate for Δ is obtained as

$$\Delta = S^{+}\Delta\Gamma \tag{38}$$

Remarks

In the present study the dynamic characteristics such as eigensolutions and FRF-s are complex valued and in numerical work it is found expeditious to separate the real and imaginary parts in equation 37 before the pseudo-inversing is done. Thus, in equation 37, by writing $\Delta\Gamma = \Delta\Gamma_R + i\Delta\Gamma_I$ and $S = S_R + iS_I$, equation 38 can be written as

$$\Delta = \begin{bmatrix} S_R \\ S_I \end{bmatrix} + \begin{Bmatrix} \Delta\Gamma_R \\ \Delta\Gamma_I \end{Bmatrix} \tag{39}$$

In equation 35, the Taylor expansion has been carried out around $\{p_u\}$ which represents the first guess on system parameters and the S matrix in equation 37 is evaluated at this initial guess. The reference value around which the Taylor expansion is done can be updated once an estimate of Δ is obtained using equation 38. This leads to an iterative strategy to solve for D as follows: $\{D\}_{\bar{k}+1} = [S]_{\bar{k}} + \{DG\}_{\bar{k}}$; $\bar{k} = 1, 2, \cdots, N_T$. This iteration could be stopped based on a suitable convergence criterion based on difference in norms of initial guess and predicted value of Δ.

A higher order system identification algorithm could be developed by retaining second and higher order terms in Taylor's expansion. Thus, in a second order method, one gets a first order sensitivity matrix $[S]^I = \left[\frac{\partial\Gamma_k}{\partial p_j}\right]$ and a second order sensitivity matrix $[S]^{II} = \left[\frac{\partial^2\Gamma_k}{\partial p_i \partial p_j}\right]$. Equation 35 here would be nonlinear in nature and these equations could be solved by combining Newton Raphson algorithm with matrix pseudo-inverse theory. The relevant details are omitted here.

Since the basic entity that is taken to be measured in the present study is a subset of the FRF matrix, it is assumed that the problem of measurement noise has been alleviated by adopting suitable band-pass filtering and adequate number of averaging.

The determination of D using equation 38 crucially depends on the matrix S being well conditioned. Often, this requirement may not be met in applications and it would become necessary to employ regularization schemes. To apply the

scheme, equation 37 is re-written as $[S^tS+\xi I]\{\Delta\} = S^t\Delta\Gamma$. Here ξ is called the regularization parameter and it is selected such that the matrix $[S^tS+\xi I]$ is not ill-conditioned. Thus, Δ is now determined using$\{\Delta\} = [S^tS+\xi I]^{-1}S^t\Delta\Gamma$. This solution can be shown as being equivalent to finding Δ such that $||S\Delta-\Delta\Gamma|| + \xi||\Delta||$ is minimized (Hansen 1994). The first term here represents the error norm and the second term the smoothness of the solution. It is clear that ξ cannot be made arbitrarily large, in which case, the physical characteristic of the original problem would be distorted; on the other hand, if ξ=0, the solution to the problem is not satisfactory, if not impossible. Thus in the selection of ξ, a trade-off is involved, and, in implementing the regularization scheme a 'L'-curve that represents $||S\Delta-\Delta\Gamma||$ versus $||\Delta||$ is constructed for different values of ξ. The value of ξ that corresponds to the knee of this curve is taken as being optimal.

5 Numerical examples

The formulations outlined in the preceding sections are illustrated in this section with the help of single and multi-dof systems. In the examples involving parameter identification, the measurement data is by and large generated synthetically except for one illustration in example 5.3 where FRF-s obtained experimentally in the laboratory have been used in system identification.

5.1 Example 1

The sdof system shown in figure 1 is considered. The system parameters assumed are m=1 kg, k=100 N/m, a_1=1 Ns/m, a= 9.2832 N/(m/s)^q, and q=3. The size of the state space is accordingly obtained as $2Nq$=6. The six eigenvalues are obtained as$-1.8487\pm0.9793i$, $-0.0358\pm2.1565i$, and $1.8845\pm1.1664i$. The corresponding right and left eigenvectors are obtained as

$$\phi = \begin{matrix} 1.3875-2.1685i & 1.3875+2.1685i & 2.1535-1.7983i \\ -1.0713+0.6055i & -1.0713-0.6055i & -0.8502-0.9845i \\ 0.5898+0.0485i & 0.5898-0.0485i & -0.4041+0.4398i \\ -0.2382-0.1525i & -0.2382+0.1525i & 0.2070+0.1839i \\ 0.0665+0.1177i & 0.0665-0.1177i & 0.0837-0.0974i \\ -0.0018-0.0646i & -0.0018+0.0646i & -0.0458-0.0380i \end{matrix}$$

$$\begin{matrix} 2.1535+1.7983i & -1.2748-2.5442i & -1.2748+2.5442i \\ -0.8502+0.9845i & -1.0933-0.6734i & -1.0933+0.6734i \\ -0.4041-0.4398i & -0.5795-0.0522i & -0.5795+0.0522i \\ 0.2070-0.1839i & -0.2347+0.1176i & -0.2347-0.1176i \\ 0.0837+0.0974i & -0.0621+0.1009i & -0.0621-0.1009i \\ -0.0458+0.0380i & 0.0001+0.0535i & 0.0001-0.0535i \end{matrix}$$

$$\psi = \begin{matrix} -0.2623+2.4986i & -0.2623-2.4986i & -2.1234+1.8257i \\ 0.6699-0.9967i & 0.6699+0.9967i & 0.8627+0.9703i \\ -0.5060+0.2711i & -0.5060-0.2711i & 0.4432-0.4074i \\ 0.2744-0.0013i & 0.2744+0.0013i & -0.1923-0.2023i \\ -0.1162-0.0608i & -0.1162+0.0608i & -0.0923+0.0907i \\ 0.0355+0.0517i & 0.0355-0.0517i & 0.0427+0.0421i \end{matrix}$$

$$\begin{matrix} -2.1234-1.8257i & 0.1931-3.2074i & 0.1931+3.2074i \\ 0.8627-0.9703i & -0.6876-1.2764i & -0.6876+1.2764i \\ 0.4432+0.4074i & -0.5669-0.3264i & -0.5669+0.3264i \\ -0.1923+0.2023i & -0.2950+0.0094i & -0.2950-0.0094i \\ -0.0923-0.0907i & -0.1110+0.0737i & -0.1110-0.0737i \\ 0.0427-0.0421i & -0.0251+0.0546i & -0.0251-0.0546i \end{matrix}$$

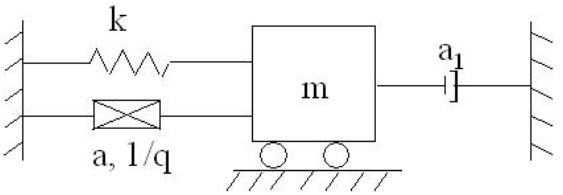

Figure 1: Sdof system considered in Example 5.1.

Figure 2 compares the FRF obtained using the direct inversion of the DSM (equation 3) with solution obtained using modal summation (equation 15 with all modes included in the summation) and, as might be expected, the two solutions show perfect mutual agreement. The application of eigenderivatives derived in section 3.2 is demonstrated by considering two models with differing model parameters as follows: Model I: m=3 kg, k=1000N/m, a=1 N/(m/s)^q, $q_=$3, and a_1=1 Ns/m; and Model II: m=3.1 kg, k=1080N/m, a=0.9 N/(m/s)^q, $q_=$3 and a_1=1 Ns/m. Table 1 shows the eigenvalues for the two models and also the prediction on the eigenvalues of Model II by using first order eigenderivative analysis on Model I. In implementing the sensitivity analysis the range of system parameters spanned by Models I and II were divided into 100 divisions. Starting from predictions from Model I, the properties of Model II were estimated by performing sensitivity analysis in 100 steps. In each step of computation an update on the initial model was obtained using first order sensitivity analysis. Similar results on the system FRF-s obtained using first order FRF sensitivity analysis are summarized in Table 2.

Figure 3 shows the results of inverse sensitivity analysis using second order eigensensitivities. Here measurements have been made on Model I and parameters to be

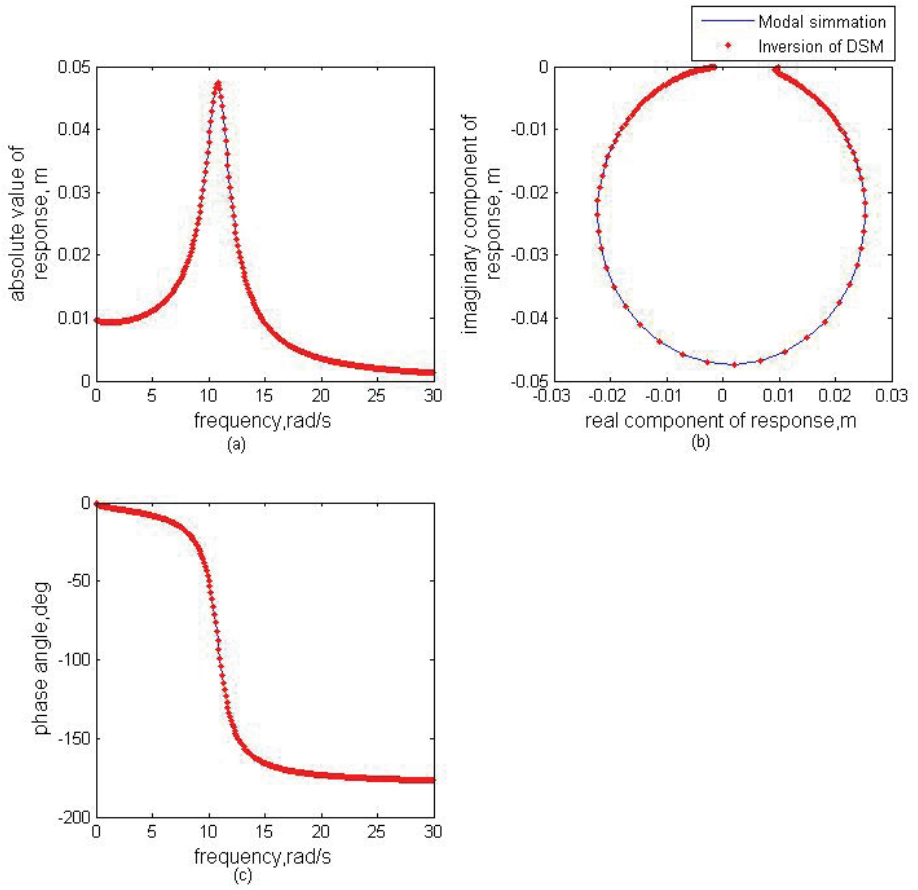

Figure 2: FRF for the Sdof system in Example 5.1 obtained using direct inversion of dynamic stiffness matrix (DSM) and by using modal summation; (a)amplitude spectrum; (b) Nyquist's plot; (c) phase spectrum.

identified are taken to be m, k and a_1. Iterations for parameter identification have been initiated with an initial guess of m=3.2 kg, k=1080 N/m and a_1= 0.9 N/(m/s)^q. It is assumed that the value of q=3 is known and hence is not treated as a parameter to be identified. This assumption is relaxed in results shown in figure 4 in which the same problem is solved using second order inverse FRF sensitivity analysis. Here the parameter q is also taken to be unknown and the initial guess on system parameters includes the guess of q =0.4 in addition to the guesses m=3.2 kg, k=1080 N/m and a_1= 0.9 N/(m/s)^q. In implementing the FRF sensitivity method a frequency range of 5 to 10 rad/s is considered and this range is divided into equi-spaced fre-

Table 1: Eigenvalues for Models I and II in example 5.1

Eigenvalue	Initial model	Direct method	Taylor's Series
λ_1	-2.3006 - 1.3188i	-2.2838 - 1.3086i	-2.2843 - 1.3089i
λ_2	-2.3006 + 1.3188i	-2.2838 + 1.3086i	-2.2843 + 1.3089i
λ_3	0.0067 - 2.6526i	0.0069 - 2.6332i	0.0069 - 2.6337i
λ_4	0.0067 + 2.6526i	0.0069 + 2.6332i	0.0069 + 2.6337i
λ_5	2.2939 - 1.3338i	2.2770 - 1.3245i	2.2774 - 1.3248i
λ_6	2.2939 + 1.3338i	2.2770 + 1.3245i	2.2774 + 1.3248i

Table 2: Results on FRF from Models I and II in example 5.1

Excitation	Response, m		
frequency (rad/s)	Initial model	Direct method	Taylor's series
10.00	0.0022 + 0.1424i	0.0019 + 0.1313i	0.0019 + 0.1317i
18.37	4.0233 - 2.0615i	5.0502 + 0.5664i	5.8385 - 0.5131i
19.00	0.2936 - 1.1653i	0.3510 - 1.2706i	0.3450 - 1.2640i
22.00	0.0115 - 0.2218i	0.0107 - 0.2138i	0.0107 - 0.2144i

quency points at an interval of 0.5 rad/s. It was observed that the Newton-Raphson iterations in implementing the second order sensitivity analysis converged in about 15 steps and a value of 0.001 was used to test the convergence of the norm of the system parameters. Thus, in this example, the two inverse sensitivity analyses procedures (based on eigensolutions and FRF-s) perform satisfactorily.

5.2 Example 2

Next, we consider the 2-dof system shown in figure 5. The governing equation for this system has the form as in equations 7 and 8. In the numerical work it is assumed that $m_1 = m_2 = 1$kg, $k_1 = k_2 = 100$N, $c_1 = 10$N/(m/s)^q; $c_2 = 0.001$Ns/m, q_1=3 and q_2=1. The size of the state space here is obtained as $2Nq$=8. The eigenvalues obtained are $-3.7872 \pm 3.8405i$, $3.7873 \pm 3.8432i$, $-1.4893 \pm 1.4773i$, $1.4893 \pm 1.5013i$/s. The results on the Nyquist plot of the FRF-s obtained using the direct inversion of the dynamic stiffness matrix (equation 3) and by using modal summation (equation 15) are shown to agree perfectly in figure 6. To demonstrate the forward and inverse sensitivity analyses we again consider two models with differing model parameters as follows: Model I: m_1=3 kg, k_1=100N/m, c_1=1.1 N/(m/s)^q, m_2= 2 kg, k_2=1000 N/m, $q_1 = 2$, $q_2 = 1$, and c_2=1 Ns/m; and Model II: m_1=3.5 kg, k_1=120N/m, c_1=0.9 N/(m/s)^q, m_2= 2 kg, k_2=1000 N/m, $q_1 = 2$, $q_2 = 1$

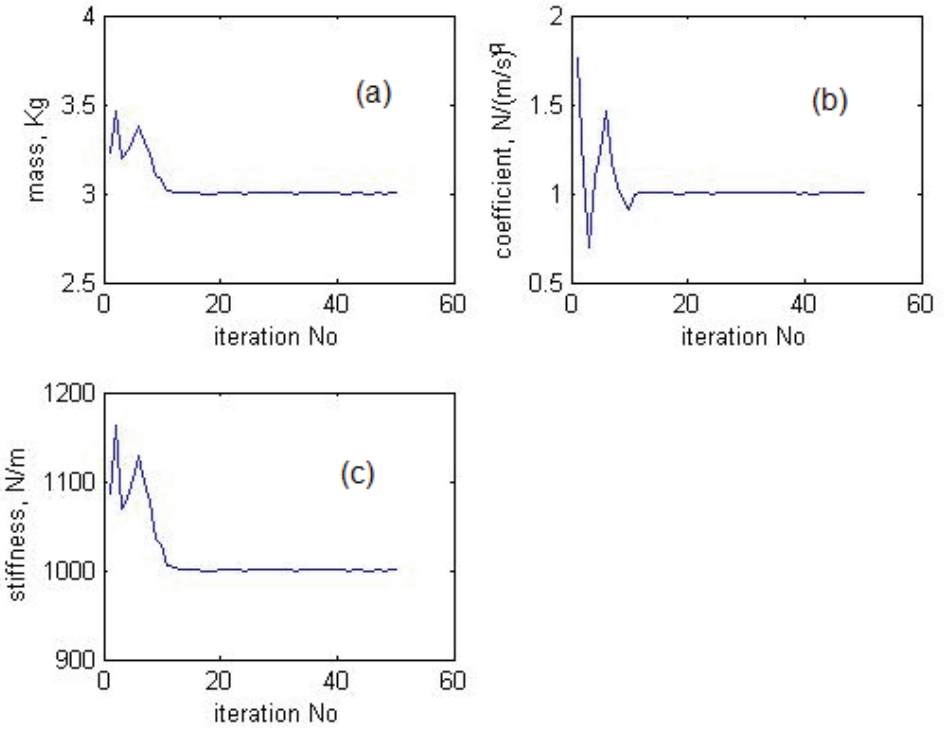

Figure 3: Parameter identification based on 2^{nd} order eigensensitivity method; example 5.1, (a) mass m, (b) damping coefficient a, and (c) stiffness k.

and c_2=1 Ns/m. The eigenvalues obtained by direct analysis and also based on the application of first order sensitivity is summarized in Table 3. In implementing the sensitivity analysis the range of system parameters spanned by Models I and II were divided into 100 divisions. Starting from predictions from Model I, the properties of Model II were estimated by performing sensitivity analysis in 100 steps. In each step of computation an update on the initial model was obtained using first order sensitivity analysis. Similar results on the system FRF-s are summarized in Table 4. The same set of models is re-considered for implementing the inverse sensitivity analysis. It is assumed that based on measurements the eigensolutions of Model II have been extracted. For the purpose of illustration it is assumed that the parameters m_2, k_2, q_1, q_2 and c_2 are known and the problem on hand consists of estimating the values of m_1, k_1 and c_1. This problem has been tackled using the second order inverse FRF sensitivity method and figure 7 shows the results obtained on the system parameters. The initial model to initiate the iterations is taken to be pro-

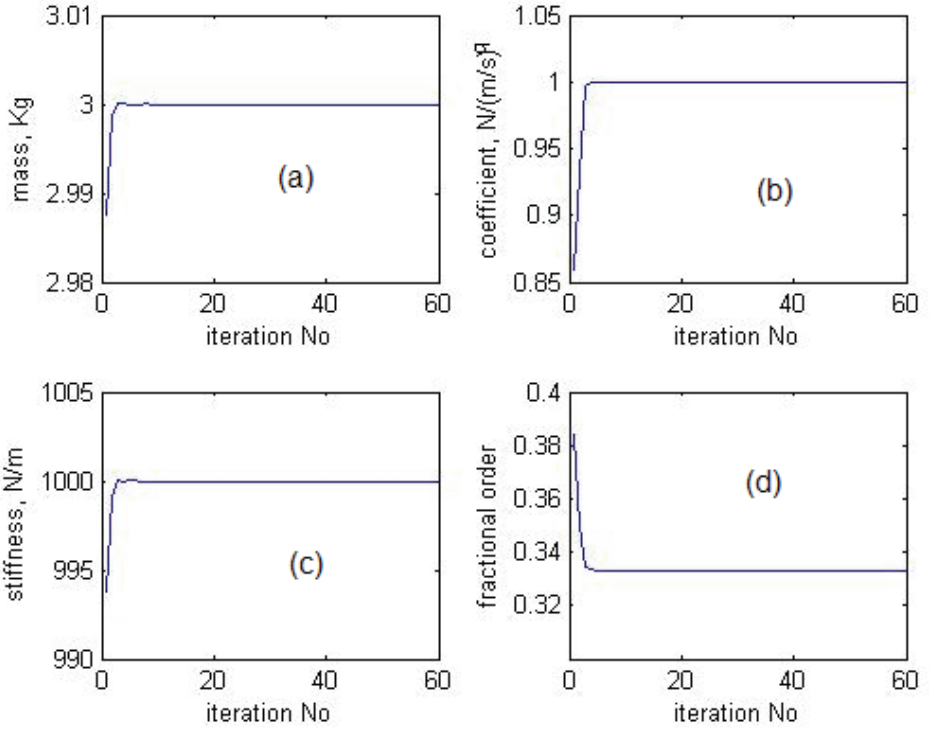

Figure 4: Parameter identification based on 2^{nd} order FRF sensitivity method for example 5.1; (a) mass m; (b) damping coefficient a; (c) stiffness k; and (d) fractional order $1/q$.

vided by Model I specified above. A frequency range of 10 rad/s to 15 rad/s with a frequency interval of 0.5 rad/s is considered for parameter identification process. Solutions were observed to converge within about 15 Newton-Raphson iterations with a value of 0.001 being used to test the convergence of the norm of the system parameters.

5.3 Example 3

Here we consider a structure made up of two steel tubes interconnected rigidly with a rubber hose and suspended freely as shown in figure 8. The steel tube has outer and inner diameters of 12.7 mm and 9.91 mm respectively, and rubber tube has diameters of 19.30 and 13.47 mm. The densities of steel and rubber were found to be respectively 8023.3 kg/m^3 and 1764.8 kg/m^3. Young's modulus of steel was taken to be 1.98E+11 Pa. With reference to the nomenclature in figure 8a, the

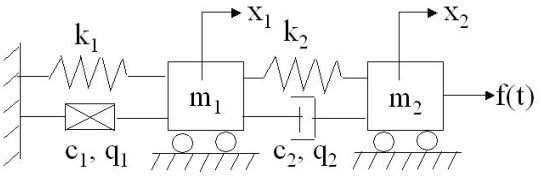

Figure 5: 2-dof system considered in example 5.2.

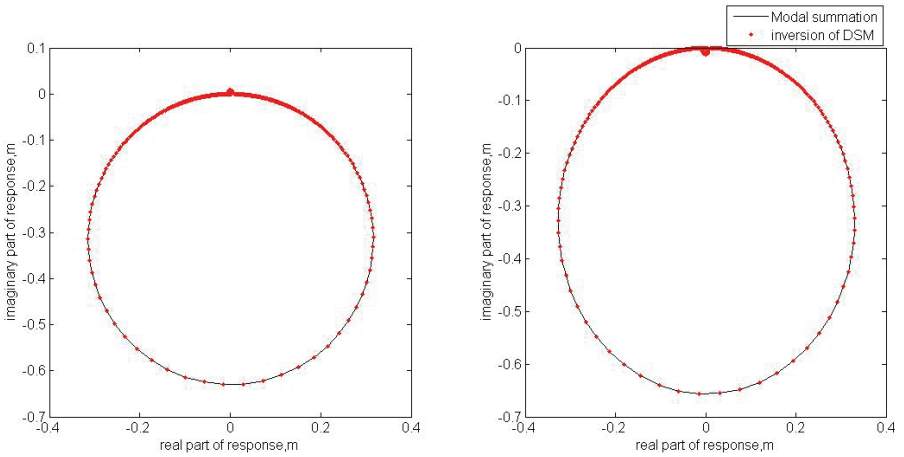

Figure 6: Nyquist's plot of FRF-s for the 2-dof system in example 5.2 obtained using direct inversion of dynamic stiffness matrix (DSM) and by using modal summation; (a) response of mass -1; (b) response of mass-2.

Table 3: Results on eigenvalues for Models I and II in example 5.2

Eigenvalue	Initial model	Direct method	Taylor's series
λ_1	-1.5220 - 1.5135i	-1.4893 - 1.4773i	-1.4912 - 1.4794i
λ_2	-1.5220 + 1.5135i	-1.4893 + 1.4773i	-1.4912 + 1.4794i
λ_3	1.5220 - 1.5306i	1.4893 - 1.5013i	1.4912 - 1.5030i
λ_4	1.5220 + 1.5306i	1.4893 + 1.5013i	1.4912 + 1.5030i
λ_5	-3.7327 - 3.7840i	-3.7872 - 3.8405i	-3.7841 - 3.8373i
λ_6	-3.7327 + 3.7840i	-3.7872 + 3.8405i	-3.7841 + 3.8373i
λ_7	3.7327 - 3.7858i	3.7873 - 3.8432i	3.7841 - 3.8398i
λ_8	3.7327 + 3.7858i	3.7873 + 3.8432i	3.7841 + 3.8398i

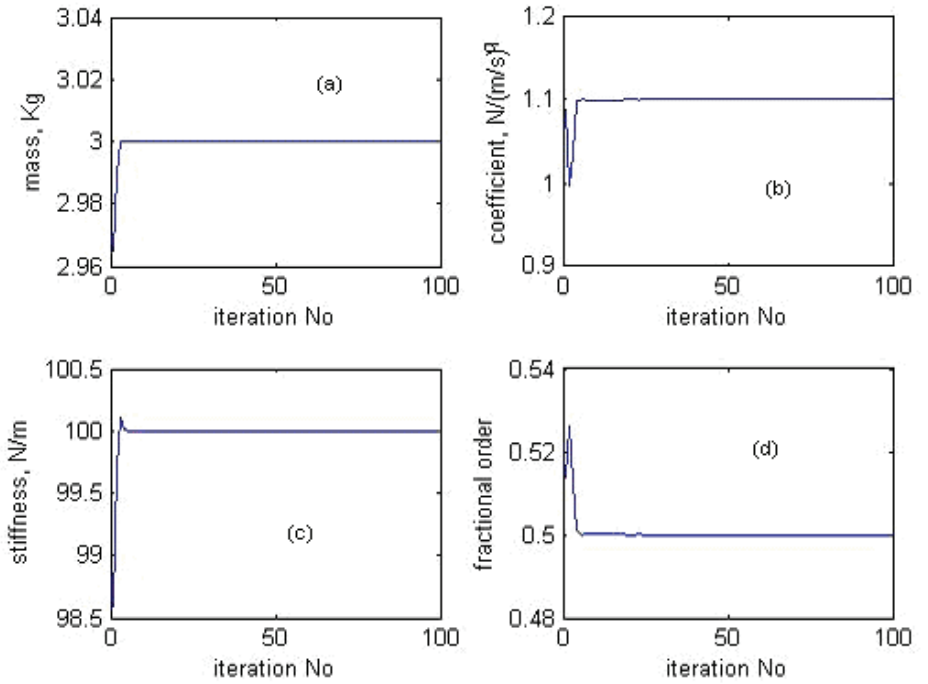

Figure 7: Parameter identification based on 2^{nd} order FRF sensitivity method for example 5.2, (a) mass, (b) damping coefficient, (c) stiffness, and (d) fractional order derivative.

structure has the following dimensions (in mm): AB=15.5, BC=95.3, CC'=20.0, C'D'=15.0, D'D=42.5, DD"=42.5, D"E'=15.0, E'E=13.3, EF=118.6 and FG=10.0 with a total length of 387.7 mm. The structure was studied both computationally and experimentally. In the computational work the structure was modeled using finite element method with 15 numbers of 2-noded Euler-Bernoulli beam elements with 2-dofs per node with spatial distribution of elements as shown in figure 8a. The stress strain relation for the rubber material here is taken to be of the form $\sigma = E\left[\varepsilon + a_1 D^{\alpha}\varepsilon\right]$ and the stiffness matrix was formulated using frequency dependent, complex valued Young's modulus (Wineman and Rajagopal 2000). Initial studies were conducted using synthetic data obtained from the numerical model. For this purpose, an initial model with E=3.4129E+07 Pa, a =0.105 N/(m/s)α and α=0.280 was used to compute the FRF-s at 20 rad/s with the drive point at F (figure 8a). The steel beams were taken to be undamped and this is considered acceptable since most of the damping in the structure is likely to originate from the rubber section.

Table 4: Results on FRF from Models I and II in example 5.1

Excitation frequency (rad/s)	Response of mass (m_1), m		
	Initial model	Direct method	Taylor's series
3	0.0438 + 1.8168i	0.0222 + 1.4284i	0.0204 + 1.4215i
4.6	4.5064 -16.1385i	12.3839 +28.0608i	24.5247 -45.2648i
5.5	0.0684 - 1.9938i	0.0669 - 2.1800i	0.0675 - 2.1527i
20	-0.0016 - 0.0980i	-0.0018 - 0.0947i	-0.0018 - 0.0955i
28.25	-0.1602 - 0.3549i	-0.8141 - 0.0540i	-0.6067 - 0.5959i
35	-0.0042 + 0.0363i	-0.0028 + 0.0277i	-0.0027 + 0.0271i
Excitation frequency (rad/s)	Response of mass (m_2), m		
	Initial model	Direct method	Taylor series
3	0.0450 + 1.9520i	0.0230 + 1.5565i	0.0213 + 1.5508i
4.6	4.7026 -16.7482i	12.9376 +29.4025i	25.5793 -47.1267i
5.5	0.0726 - 2.0158i	0.0711 - 2.2140i	0.0717 - 2.1847i
20	0.0026 + 0.0094i	0.0032 + 0.0261i	0.0031 + 0.0249i
28.25	0.2307 + 0.4462i	1.3618 + 0.0260i	0.8995 + 0.8593i
35	0.0060 - 0.0938i	0.0047 - 0.0879i	0.0048 - 0.0880i

Furthermore, by using first order sensitivity, the FRF-s at the same frequency and at all the nodes in the finite element model were computed for a modified system with E=3.61975E+07 Pa, a =0.125 N/(m/s)α and α=0.225. The results of this forward sensitivity analysis are compared with the exact FRF-s for the modified system in Table 5. The two results show satisfactory mutual agreement. Results of a second order inverse sensitivity analysis to identify E, a and α of the rubber tube are shown in figure 9. Here 'measurements' on system FRF-s were synthetically simulated (with drive point at F) over a frequency range of 879.64 rad/s (140 Hz) to 917.34 rad/s (146 Hz) for a system with E=3.61975E+07 Pa, a =0.125 N/(m/s)α and α=0.225. This frequency range was divided into 12 points in implementing the inverse FRF sensitivity analysis. The iterations were initiated with an initial model with E=3.4129E+07 Pa, a =0.105 N/(m/s)$^{\alpha}$ and α=0.280. It may be observed from figure 9 that the estimated parameters show satisfactory convergence after about 40 iterations.

With a view to assess the performance of the identification procedure when measured data are obtained in a laboratory experiment, the set up shown in figure 8c was used to measure FRF-s with driving via a modal shaker at point F as shown. The response of the beam structure was measured using five accelerometers and the applied force was measured using a force transducer as shown in figure 8b.

Table 5: Forward sensitivity analysis on FRF at 20 rad/s for the system in example 5.3

Degree of freedom	Response, (m)		
	Initial model	Direct method	Taylor series
1	0.0015 - 0.0011i	0.0022 - 0.0014i	0.0022 - 0.0013i
2	-0.0004 + 0.0003i	-0.0005 + 0.0003i	-0.0005 + 0.0003i
3	0.0012 - 0.0009i	0.0018 - 0.0011i	0.0018 - 0.0011i
4	-0.0004 + 0.0003i	-0.0005 + 0.0003i	-0.0005 + 0.0003i
5	0.0012 - 0.0009i	0.0018 - 0.0011i	0.0018 - 0.0011i
6	-0.0004 + 0.0003i	-0.0005 + 0.0003i	-0.0005 + 0.0003i
7	-0.0001 + 0.0001i	-0.0001 + 0.0001i	-0.0001 + 0.0001i
8	-0.0004 + 0.0003i	-0.0005 + 0.0003i	-0.0005 + 0.0003i
9	-0.0001 + 0.0001i	-0.0002 + 0.0002i	-0.0002 + 0.0002i
10	-0.0004 + 0.0003i	-0.0005 + 0.0003i	-0.0005 + 0.0003i
11	-0.0004 + 0.0003i	-0.0006 + 0.0004i	-0.0006 + 0.0004i
12	-0.0004 + 0.0003i	-0.0005 + 0.0003i	-0.0005 + 0.0003i
13	-0.0006 + 0.0005i	-0.0009 + 0.0006i	-0.0009 + 0.0006i
14	-0.0004 + 0.0003i	-0.0005 + 0.0003i	-0.0005 + 0.0003i
15	-0.0009 + 0.0007i	-0.0014 + 0.0009i	-0.0014 + 0.0009i
16	-0.0000 - 0.0000i	-0.0001 + 0.0000i	-0.0001 + 0.0000i
17	-0.0009 + 0.0007i	-0.0014 + 0.0009i	-0.0014 + 0.0009i
18	-0.0000 - 0.0000i	-0.0001 - 0.0000i	-0.0001 - 0.0000i
19	-0.0007 + 0.0005i	-0.0011 + 0.0006i	-0.0011 + 0.0006i
20	0.0003 - 0.0003i	0.0004 - 0.0003i	0.0004 - 0.0003i
21	-0.0006 + 0.0003i	-0.0008 + 0.0004i	-0.0008 + 0.0004i
22	0.0003 - 0.0003i	0.0004 - 0.0003i	0.0004 - 0.0003i
23	-0.0004 + 0.0002i	-0.0006 + 0.0002i	-0.0006 + 0.0002i
24	0.0003 - 0.0003i	0.0004 - 0.0003i	0.0004 - 0.0003i
25	-0.0004 + 0.0002i	-0.0006 + 0.0002i	-0.0006 + 0.0002i
26	0.0003 - 0.0003i	0.0004 - 0.0003i	0.0004 - 0.0003i
27	0.0009 - 0.0012i	0.0013 - 0.0013i	0.0014 - 0.0013i
28	0.0003 - 0.0003i	0.0004 - 0.0003i	0.0004 - 0.0003i
29	0.0009 - 0.0012i	0.0014 - 0.0014i	0.0014 - 0.0014i
30	0.0003 - 0.0003i	0.0004 - 0.0003i	0.0004 - 0.0003i
31	0.0010 - 0.0013i	0.0015 - 0.0015i	0.0015 - 0.0015i
32	0.0003 - 0.0003i	0.0004 - 0.0003i	0.0004 - 0.0003i
33	0.0009 + 0.0496i	0.0014 + 0.0494i	0.0014 + 0.0494i

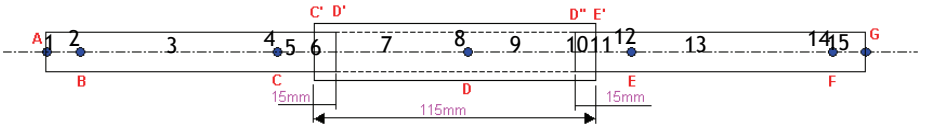

(a)

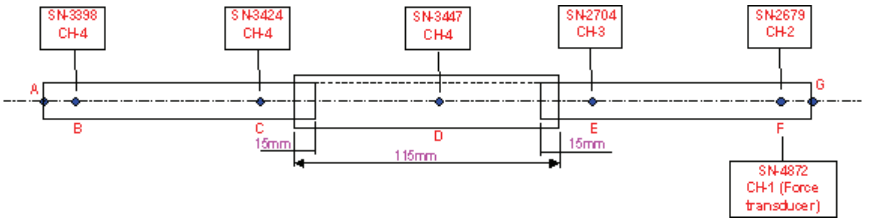

(b)

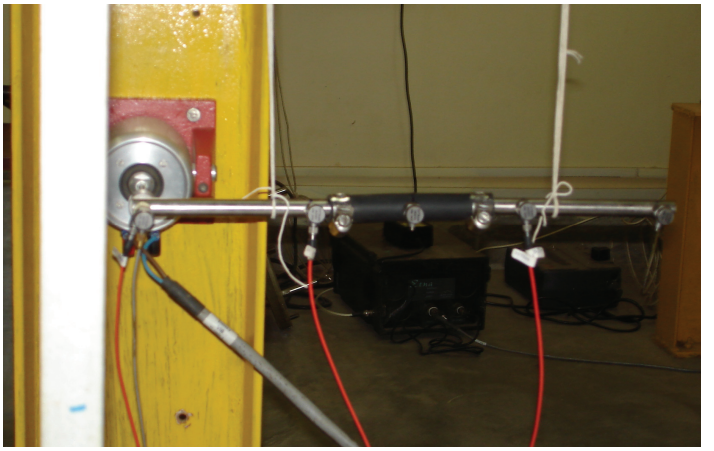

(c)

Figure 8: Steel and rubber pipe structure considered in example 5.3; (a) details of nodes in finite element model; (b) details of sensor deployment; (c) experimental setup.

Following standard procedures for measurement of FRF-s (McConnel 1995) and using 500 number of averages, the system FRF-s were measured; some of these measurements are shown in figure 10. This figure shows three episodes of measurements with each episode involving averaging across 500 samples. The results shown confirm satisfactory repeatability of the measurements. By selecting the frequency range of 122.62 to 124.45 Hz, and, with 31 number of frequency points,

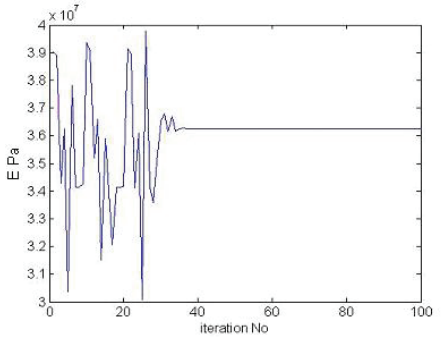

(a)

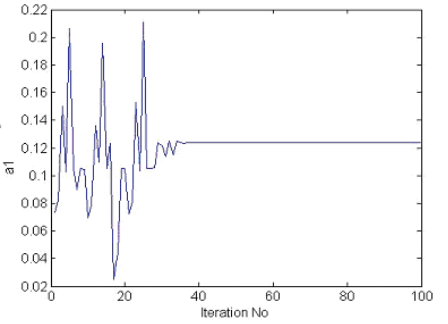

(b)

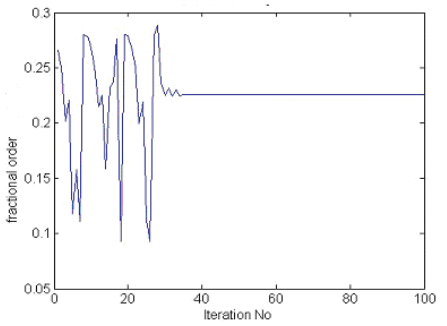

(c)

Figure 9: Parameter identification based on 2^{nd} order FRF sensitivity method for example 5.3 based on synthetic data, (a) Young's modulus, (b) damping coefficient, (c) fractional order derivative.

the second order inverse FRF sensitivity analysis was implemented to estimate E, a and α of the rubber material. The Young's modulus of steel material was assumed to be known (E=1.98E+11 Pa). Figure 11 shows the results on identification of Young's modulus of rubber segment and damping parameters. The system parameters showed minor oscillations that remained bounded as iterations proceeded. The results in the last few iterations were averaged to obtain the estimates: E= 3.5987e+07Pa, a=0.1246 N/(m/s)α, and α =0.22. Using these parameters a few of the FRF-s were reconstructed and compared with measurements and these results are shown in figure 12. The identification procedure was observed to be not uni-

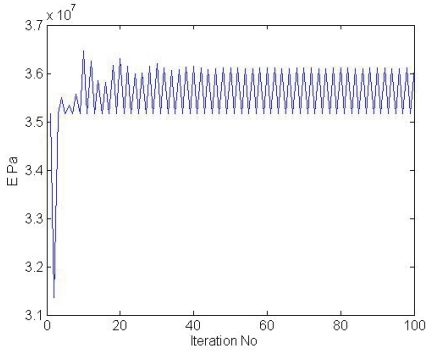

(a)

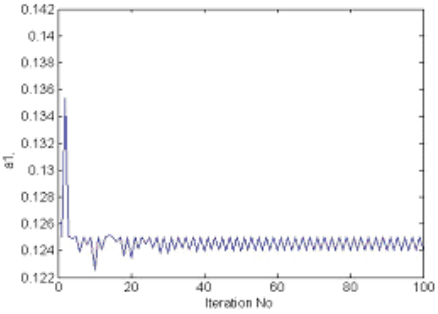

(b)

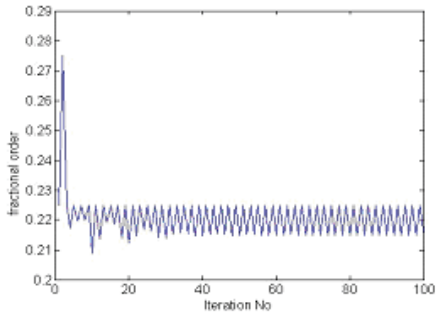

(c)

Figure 10: Parameter identification based on 2^{nd} order FRF sensitivity method for example 5.3 based on experimental data, (a) Young's modulus, (b) damping coefficient, (c) fractional order derivative.

formly successful with the method performing poorly especially in low frequency ranges. The success of method was seen to depend upon the choice of frequency points to be included in the identification procedure. Further work is needed in establishing criteria for selecting the frequency points bearing in mind the quality of FRF measurements as indicated by departure of the spectrum of coherence function deviating from the expected value of unity.

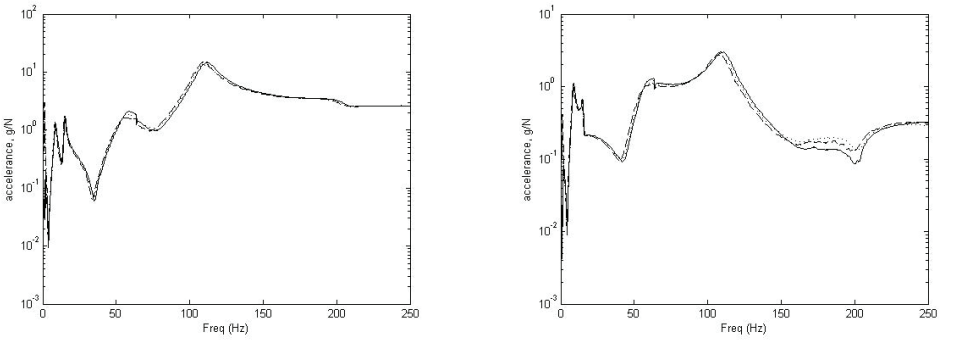

(a) (b)

Figure 11: Measured accelerance for the system shown in figure 8c; (a) accelerance at the drive point; (b) accelerance at E; results three episodes of measurements with each involving averaging across 500 samples are shown here.

6 Closing remarks

The use of fractional order derivatives in modeling the constitutive behavior of visco-elastic materials is well investigated in the existing literature. Studies on identifying parameters of dynamical systems with visco-elastic structural elements are however not widely available. This paper has explored the applicability of inverse sensitivity methods based on system eigensolutions and frequency response functions for identifying mass, stiffness and dissipation characteristics of systems governed by fractional order differential equations. The following concluding remarks are made based on this study:

- The application of inverse eigensolutions method requires the problem to formulated in a state space form with the size of this model depending upon the value of the fractional order α. The formulation is possible when α is a rational number and, for $\alpha = 1/q$, with q being an integer; the size of the state space is $2Nq$. The computational effort involved in system identification depends this size, which in turn, somewhat artificially depends on the parameter q. Furthermore, if q itself is a parameter to be identified, the method based on eigensolutions becomes difficult to apply. Also, this method requires that the eigensolutions of the system have been already extracted based on the measured FRF-s before the parameter identification problem could be tackled. Given that the eigensolutions here are governed by asymmetric generalized, eigenvalue problem, this extraction is not straightforward. The experimental

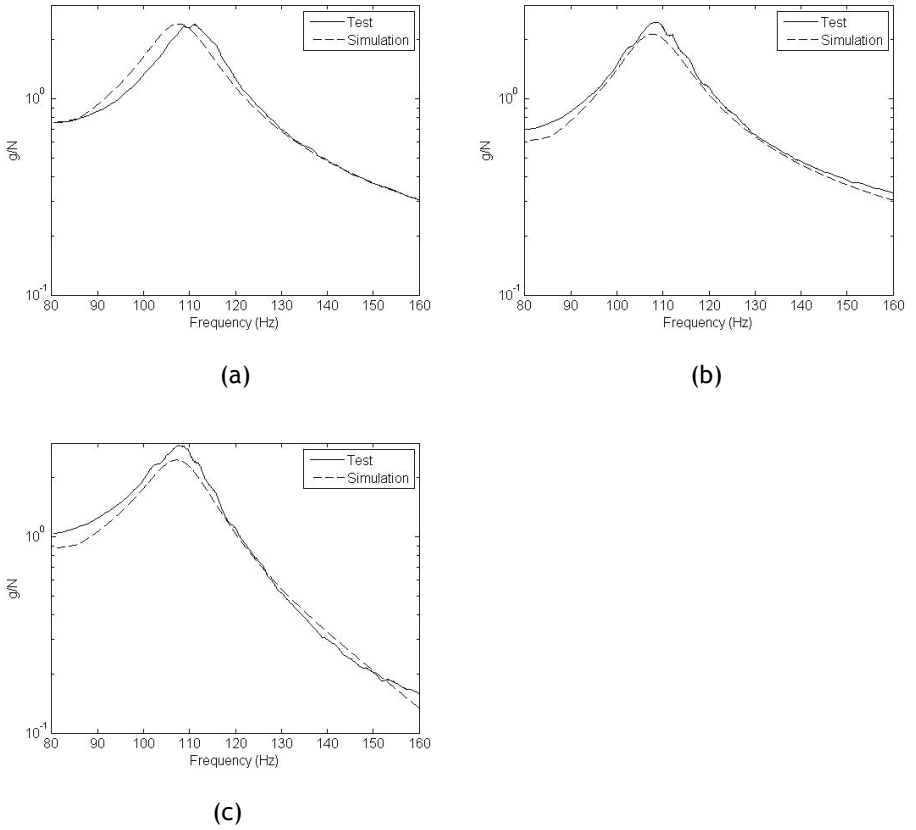

Figure 12: Example 5.3; Comparison of accelerance at sensor locations B,C and E (figure 8) from measurements (Test) and from results of system identification (Simulation); (a) location B; (b) location C; and (c) location E.

modal analysis procedures in this context are presently not fully developed in the existing literature.

- The method based on inverse sensitivity analysis of FRF-s is better suited in this context since it does not suffer from the above mentioned drawbacks of the eigensolutions method. The size of the FRF matrix is not dependent on order of the fractional derivative. This method permits the fractional order itself to be a parameter to be identified and is based on primary response variables (*viz*, the FRF-s) that are experimentally measured.

- Further work is needed to establish criteria for selecting number of frequency

points to be included in the FRF based identification method. The measured data reduction based on singular value decomposition of the FRF matrix (as has been recently proposed by Venkatesha *et al*, 2008 for the identification of viscously damped systems) could offer means to reduce the number of equations to be tackled.

References

Adhikari S. (2002): Dynamics of non-viscously damped linear systems, *ASCE Journal of Engineering Mechanics*, 128(3), 328-339.

Adhikari S. (2005): Qualitative dynamic characteristics of non-viscously damped oscillator, *Proceedings of Royal Society of London A*, 461, 2059, 2269-2288.

Agrawal O. P. Analytical solution for stochastic response of a fractionally damped beam, *ASME Journal of Vibration and Acoustics*, 126, 561-566.

Bagley R. L., Torvic P. J. (1983a): Fractional calculus- a different approach to the analysis of visco-elastically damped structures, *AIAA Journal*, 21(5), 741-748.

Bagley R. L., Torvic P. J. (1983b): A theoretical basis for the application of fractional calculus viscoelasticity, *Journal of Rheology*, 27(3), 203-210.

Choi K. M., Cho S. W., Ko M. G., Lee I. W. (2004): Higher order eigensensitivity analysis of damped systems with repeated eigenvalues, *Computers and Structures*, 82, 63-69.

Choi K. M., Cho S. W., Ko M. G., Lee I. W. (2004): Sensitivity analysis of nonconservative eigensystems, *Journal of Sound and Vibration*, 274, 997-1011.

Ewins D. J. (2000): *Modal testing: Theory, Practice and Application*, Research studies press limited, Baldock, Hertfordshire.

Hansen P. C. (1994): Regularization tools: A Matlab package for analysis and solution of discrete ill-posed problems, *Numerical Algorithms*, 6, 1–35.

Huang C. H., Shih C. C. (2007): An inverse problem in estimating simultaneously the time dependent applied force and moment of an Euler-Bernoulli beam, *CMES: Computer Modeling in Engineering and Sciences*, 21(3), 239-254, 2007.

Huang C. H., Shih C. C. (2007): An inverse problem in estimating simultaneously the time dependent applied force and moment of an Euler-Bernoulli beam, *CMES: Computer Modeling in Engineering and Sciences*, 21(3), 239-254, 2007.

Ingman D., Suzdalnitsky J. (2001): Iteration method for equation of viscoelastic motion with fractional differential operator damping, *Computer methods in applied mechanics and engineering*, 190, 5027-5036.

Jones D. I. G. (2001): *Handbook of viscoelastic vibration damping*, John Wiley

& Sons, Chichester.

Lee J. H., Kim J, (2001): Identification of damping matrices from measured frequency response functions, *Journal of Sound and Vibration*, 240(3), 545-565.

Lee H. H., Tsai C. S. (1994): Analytical model for viscoelastic dampers for seismic mitigation of structures, *Computers and Structures*, 50(1), 111-121.

Lin R. M., Lim M. K., Du H. (1994): A new complex inverse eigensensitivity method for structural damping model identification, *Computers and Structures*, 52(5), 905-915.

Lin R. M., Lim M. K., Du H. (1995): Improved inverse eigensensitivity method for structural analytical model updating, Transactions of ASME, *Journal of Vibration and Acoustics*, 117,192-198.

Maia N. M. M., Silva J. M. M, (1997): *Theoretical and experimental modal analysis*, Research Studies Press Limited, Taunton, Somerset, England.

Maia N. M. M, Silva J. M. M., Almas E. A. M, (2003): Damage detection in structures: From mode shape to frequency response function methods, *Mechanical Systems and Signal Processing*, 17(3), 489-498.

Maia N. M. M, Silva J. M. M., Riberio A. M. R. (1998): On a general model for damping, *Journal of Sound and Vibration*, 218(5), 749-767.

Mallik A. K. (1990): *Principles of vibration control*, Affiliated East-West Press, New Delhi.

McConnel (1995): *Vibration testing: Theory and practice*, John Wiley, New York.

Mead D. J. (2000): *Passive vibration control*, John Wiley & Sons, Chichester.

Muhr A. H. (2007): Mechanics of elastomer-shim laminates, *CMC: Computers, Materials and Continua*, vol.5, no.1, pp.11-29, 2007

Nashif A. D., Jones D. I. G., Hendersen J. P. *Vibration damping*, John Wiley & Sons, New York.

Oldham K. B., Spanier J. (1974): *The fractional calculus*, Academic Press, New York.

Pritz T. (1996): Analysis of four-parameter fractional derivative model of real solid materials, *Journal of Sound and vibration*, 195, 103-115.

Ray S. S., Poddar B. P., Bera R. K. (2005): Analytical solution of a dynamic system containing fractional derivative of order one-half by Adomian decomposition method, *Journal of Applied Mechanics*, 72, 290-295.

Reddy K. V., Ganguli R. (2007): Fourier analysis of mode shapes of damaged beams, *CMC: Computers, Materials and Continua*, 5(2), 79-98.

Sivaprasad R. (2008): *Steady state vibration analysis of structures with viscoelas-*

tic components, MSc (Engg) thesis to be submitted, Department of Civil Engineering, Indian Institute of Science, Bangalore.

Spanos P. D., Zeldin B. A. (1997): Random vibration of systems with frequency dependent parameters or fractional derivatives, *ASCE Journal of Engineering Mechanics*, 123(3), 290-292.

Tabrez S., Mitra M., Gopalakrishnan S. (2007): Modeling of degraded composite beam due to moisture absorption for wave based detection, *CMES: Computer Modeling in Engineering and Sciences*, 22(1), 77-90.

Venkatesha S. (2007): *Inverse sensitivity methods in linear structural damage detection using vibration data*, MSc (Engg.) Thesis, Department of Civil Engineering, Indian Institute of Science, Bangalore, India.

Venkatesha S., Rajender R., Manohar C. S. (2008): Inverse sensitivity analysis of singular solutions of FRF matrix in structural system identification, *CMES: Computer Modeling in Engineering and Sciences*, 37(2), 113-152.

Wineman A. S., Rajagopal K. R. (2000): *Mechanical response of polymers*, Cambridge University Press, Cambridge.

Woodhouse J. (1998): Linear damping models for structural vibrations, *Journal of Sound and Vibration*, 215(3), 547-569.